Stochastic transport of interacting particles in periodically driven ratchets

Sergey Savel'ev,[1] Fabio Marchesoni,[1,2] and Franco Nori[1,3]
[1]*Frontier Research System, The Institute of Physical and Chemical Research (RIKEN), Wako-shi, Saitama 351-0198, Japan*
[2]*Dipartimento di Fisica, Universitá di Camerino, I-62032 Camerino, Italy*
[3]*Center for Theoretical Physics, Department of Physics, University of Michigan, Ann Arbor, Michigan 48109-1120, USA*
(Received 2 May 2004; revised manuscript received 2 September 2004; published 23 December 2004)

An open system of overdamped, interacting Brownian particles diffusing on a periodic substrate potential $\mathcal{U}(x+l)=\mathcal{U}(x)$ is studied in terms of an infinite set of coupled partial differential equations describing the time evolution of the relevant many-particle distribution functions. In the mean-field approximation, this hierarchy of equations can be replaced by a nonlinear integro-differential Fokker-Planck equation. This is applicable when the distance a between particles is much less than the interaction length λ, i.e., a particle interacts with many others, resulting in averaging out fluctuations. The equation obtained in the mean-field approximation is applied to an ensemble of locally ($a \ll \lambda \ll l$) interacting (either repelling or attracting) particles placed in an asymmetric one-dimensional substrate potential, either with an oscillating temperature (temperature rachet) or driven by an ac force (rocked ratchet). In both cases we focus on the high-frequency limit. For the temperature ratchet, we find that the net current is typically suppressed (or can even be inverted) with increasing density of the repelling particles. In contrast, the net current through a rocked ratchet can be enhanced by increasing the density of the repelling particles. In the case of attracting particles, our perturbation technique is valid up to a critical value of the particle density, above which a finite fraction of the particles starts condensing in a liquidlike state near the substrate minima. The dependence of the net transport current on the particle density and the interparticle potential is analyzed in detail for different values of the ratchet parameters.

DOI: 10.1103/PhysRevE.70.061107 PACS number(s): 05.40.Jc, 87.16.Uv

I. INTRODUCTION

The transport of particles moving out of equilibrium in an asymmetric substrate potential has been studied intensively for a variety of different systems [1,2] in order to achieve an efficient control of the net particle flow. Various realizations of rachet systems working out of equilibrium have been proposed involving different rectification mechanisms, like temporal temperature oscillations (temperature ratchet [3]), zero-average sinusoidal ac forces (ac tilted or rocked ratchet [4]), stochastic and deterministic fluctuations of the ratchet potentials [5], among others. The ensuing net dc drift (the so-called ratchet current or rectification effect) occurring in these systems is important for several biological motors as well as for some technological applications; e.g., for particle separation techniques [6], smoothing of atomic surface during electromigration [7], and superconducting vortex motion control [8,9].

The dc particle current can be controlled to some extent and even inverted, for instance, by changing the frequency of the ac drive or tinkering with the shape of the asymmetric potential [1,2,10]—neither one a simple procedure under many experimental circumstances. Indeed most asymmetric substrates are fixed. Moreover, until recently [11,12], interparticle *interactions*, a central feature in most physical systems, have been neglected in almost all theoretical studies on ratchet transport [13] or, on rare occasions, only tackled numerically [8,14]. For instance, one-dimensional (1D) numerical simulations [14] of an assembly of hard-core rods show quite unusual stochastic transport properties, including current inversion with varying particle density and commensurability effects when the ratio of the particle size to the substrate unit length is a rational number. It follows that many important phenomena such as *dynamical phase transitions*, as well as *competition between thermal fluctuations and particle-particle interaction in stochastic transport*, have not yet been investigated analytically. This is a major limitation imposed by the key theoretical tool employed by most authors, namely, the linear Fokker-Planck equation, which describes well only the nonequilibrium diffusion of a single Brownian particle or, equivalently, of a system of noninteracting particles. Therefore, this fundamental equation must be generalized to address the transport properties of interacting particles.

On combining stochastic and Bogoliubov kinetic techniques, in Sec. II we develop a closed-form statistical approach based on many-particle distribution functions, to describe the net transport of interacting particles moving on periodic asymmetric substrates subject to fluctuating forces. In the mean-field approximation, where a two-particle distribution function is approximated by the product of the two relevant one-particle distributions, a nonlinear Fokker-Planck equation is derived. We apply this equation to a system of locally interacting particles, which is kept out of equilibrium by high-frequency oscillations of either the temperature or an external deterministic ac force.

For the case of *repelling* particles in a temperature ratchet (Sec. III), the net particle drift is *suppressed* when raising the particle density. In contrast, the rectified current of a rocked ratchet (Sec. IV) *increases* with the density of the repelling particles as long as the drive amplitude is relatively small.

In the case of *attracting* particles, the perturbation approach of Sec. II applies for increasing particle densities until the particles start *condensing* in the potential wells. The net particle velocity diminishes with increasing particle density for both the temperature ratchets and the rocked ratchets

driven at small ac amplitude. However, the drift current through a rocked ratchet can be strongly enhanced with increasing particle density at larger drive amplitudes (Sec. IV).

Such an unusual behavior can be qualitatively explained in terms of the flattening of the asymmetric effective potential acting on the repelling particles and the deepening of the effective potential wells binding the attracting particles. These opposite mechanisms suggest *an efficient control of the ratchet rectification process by tuning the density of the interacting particles*. The latter has recently been experimentally implemented for the control of the motion of superconducting vortices in microstructures [15].

II. THERMAL DIFFUSION OF INTERACTING PARTICLES

A. Temporal evolution of many-particle distributions

Let us consider an open system of N pointlike Brownian particles interacting with each other via the pairwise potential $\mathcal{W}$, with the substrate through the asymmetric periodic potential $\mathcal{U}$, and with a homogeneous external field corresponding to the time-dependent deterministic force $\vec{F}(t)$. The environment exerts on each particle an independent Gaussian random force with zero mean and intensity controlled by the temperature T. In the overdamped regime (where inertia is negligible compared to the viscous damping), the Langevin equation describing the thermal diffusion of the ith particle is

$$\eta\dot{\vec{x}}_i = -\frac{\partial\mathcal{U}(\vec{x}_i)}{\partial\vec{x}_i} - \sum_{j\neq i}\frac{\partial}{\partial\vec{x}_i}\mathcal{W}(\vec{x}_i-\vec{x}_j) + \vec{F}(t) + \sqrt{2\eta k_B T}\vec{\xi}^{(i)}(t), \tag{1}$$

where $\vec{x}_i(t)=(x_i(t),y_i(t),z_i(t))$ is the position of the ith particle at time t, $\vec{\xi}^{(i)}=(\xi_x^{(i)}(t),\xi_y^{(i)}(t),\xi_z^{(i)}(t))$ is the random force acting on it, $\dot{\vec{x}}_i \equiv d\vec{x}_i/dt$, η is the viscous coefficient, and k_B is the Boltzmann constant. We further assume the fluctuation-dissipation relation $\langle\xi_\alpha^{(i)}(0)\xi_\beta^{(j)}(t)\rangle=\delta(t)\delta_{\alpha\beta}\delta_{i,j}$, where $\delta(t)$ is the Dirac δ function, and $\delta_{\alpha\beta}$ and $\delta_{i,j}$ are Kronecker symbols.

This set of dynamical equations has been effectively simulated in several numerical studies (see, for instance, Ref. [8]). It takes some nontrivial algebraic manipulations to cast them in an analytically tractable form. For this purpose let us consider the time evolution of the microscopic particle distribution $\mathcal{N}_1=\Sigma_i\delta(\vec{x}-\vec{x}_i(t))$; for a small time increment Δt,

$$\begin{aligned}\mathcal{N}_1(t+\Delta t) &= \sum_i \delta(\vec{x}-\vec{x}_i(t+\Delta t)) = \sum_i \delta(\vec{x}-\vec{x}_i(t)-\dot{\vec{x}}\Delta t)\\ &\approx \sum_i \delta(\vec{x}-\vec{x}_i(t)) - \sum_i \frac{\partial\delta(\vec{x}-\vec{x}_i(t))}{\partial\vec{x}}\dot{\vec{x}}\Delta t\\ &\quad + \frac{k_B T}{\eta}\sum_i \frac{\partial\delta(\vec{x}-\vec{x}_i(t))}{\partial x_\alpha\partial x_\beta}\xi_\alpha^{(i)}\xi_\beta^{(i)}(\Delta t)^2,\end{aligned} \tag{2}$$

where summation over repeated indices α, β is understood. Averaging over the stochastic variables $\vec{\xi}^{(i)}$ and inserting the identities $\langle\xi_\alpha^{(i)}\rangle=0$ and $\langle\xi_\alpha^{(i)}\xi_\beta^{(i)}\rangle=\delta_{\alpha\beta}/\Delta t$ yields

$$\begin{aligned}&\frac{\eta}{\Delta t}[\mathcal{N}_1(t+\Delta t)-\mathcal{N}_1(t)]\\ &\quad = \frac{\eta}{\Delta t}\left(\sum_i \delta(\vec{x}-\vec{x}_i(t+\Delta t)) - \sum_i \delta(\vec{x}-\vec{x}_i(t))\right)\\ &\quad \approx \frac{\partial}{\partial\vec{x}}\sum_i \delta(\vec{x}-\vec{x}_i)\left(\frac{\partial\mathcal{U}(\vec{x}_i)}{\partial\vec{x}_i} + \sum_{j\neq i}\frac{\partial}{\partial\vec{x}_i}\mathcal{W}(\vec{x}_i-\vec{x}_j) - \vec{F}(t)\right)\\ &\qquad + k_B T\frac{\partial^2}{\partial x_\alpha\partial x_\alpha}\sum_i \delta(\vec{x}-\vec{x}_i).\end{aligned} \tag{3}$$

Note that in Eq. (2) we have retained the stochastic contributions up to second order in Δt. However, after averaging over noise, such apparently next-to-leading corrections generate additional first order terms in Eq. (3). The reason for that is the δ-like noise autocorrelation function, which, in view of the time discretization, corresponds to a zero-mean stochastic noise with amplitude of the order of $\sqrt{2k_B\eta T/\Delta t}$. Physically, Δt can be regarded as the smallest time scale in the problem, say, the mean collisional time of the particle gas. In the limit $\Delta t\to 0$ the amplitude of the random force diverges, keeping the quantity $\langle\xi_\alpha^{(i)}\xi_\beta^{(i)}\rangle\Delta t$ constant [16].

In order to treat the particle motion as a stochastic process, we introduce the set of many-particle distributions $F_1(t,\vec{x}_1)$, $F_2(t,\vec{x}_1,\vec{x}_2),\ldots,F_N(t,\vec{x}_1,\ldots,\vec{x}_N)$. Here, the s-particle distribution $F_s(t,\vec{x}_1,\ldots,\vec{x}_s)$ defines the particle number density for *any* s, with $s\leqslant N$, elemental volumes $[\vec{x}_1,\vec{x}_1+d\vec{x}_1],\ldots,[\vec{x}_s,\vec{x}_s+d\vec{x}_s]$ at time t. On normalizing each F_s to the number $N(N-1)\cdots(N-s+1)$, one obtains an identity relating F_s to F_{s-1}, i.e.,

$$F_{s-1}(t,\vec{x}_1,\ldots,\vec{x}_{s-1}) = \frac{1}{N-s+1}\int d\vec{x}_s F_s(t,\vec{x}_1,\ldots,\vec{x}_s), \tag{4}$$

with $F_0\equiv 1$ and the spatial integration taken over the whole space accessible to the particles. Multiplying Eq. (3) by F_N and integrating over all variables $\vec{x}_1,\ldots,\vec{x}_N$ lead to the following equation for the one-particle distribution function F_1:

$$\begin{aligned}\eta\frac{\partial F_1(t,\vec{x})}{\partial t} &= \frac{\partial}{\partial\vec{x}}\left[\left(\frac{\partial\mathcal{U}(\vec{x})}{\partial\vec{x}} - \vec{F}(t)\right)F_1(t,\vec{x})\right]\\ &\quad + \frac{\partial}{\partial\vec{x}}\int d\vec{x}' F_2(t,\vec{x},\vec{x}')\frac{\partial\mathcal{W}(\vec{x}-\vec{x}')}{\partial\vec{x}}\\ &\quad + k_B T\frac{\partial^2 F_1(t,\vec{x})}{\partial x_\alpha\partial x_\alpha}.\end{aligned} \tag{5}$$

This equation for $F_1(t,\vec{x})$ does not completely specify $F_1(t,\vec{x})$, because the interaction term involves the pair distribution function $F_2(t,\vec{x},\vec{x}')$. The required additional equation for F_2 may be derived by considering the time evolution of the microscopic pair function $\mathcal{N}_2=\Sigma_{i\neq j}\delta(\vec{x}-\vec{x}_i(t))\delta(\vec{x}'-\vec{x}_j(t))$. Following the approach (2)–(5) outlined above, the equation for the evolution of the $\mathcal{N}_2$ can be written as

$$\frac{\eta}{\Delta t}[\mathcal{N}_2(t+\Delta t)-\mathcal{N}_2(t)]$$
$$=\frac{\partial}{\partial \vec{x}}\Bigg[\sum_{i\neq j}\delta(\vec{x}-\vec{x}_j)\delta(\vec{x}'-\vec{x}_j)\times\left(\frac{\partial \mathcal{U}(\vec{x}_i)}{\partial \vec{x}_i}+\sum_{l\neq i}\frac{\partial \mathcal{W}(\vec{x}_i-\vec{x}_l)}{\partial \vec{x}_i}-\vec{F}(t)\right)\Bigg]$$
$$+\frac{\partial}{\partial \vec{x}'}\Bigg[\sum_{i\neq j}\delta(\vec{x}-\vec{x}_i)\delta(\vec{x}'-\vec{x}_j)\times\left(\frac{\partial \mathcal{U}(\vec{x}_j)}{\partial \vec{x}_j}+\sum_{l\neq j}\frac{\partial \mathcal{W}(\vec{x}_j-\vec{x}_l)}{\partial \vec{x}_j}-\vec{F}(t)\right)\Bigg]$$
$$+k_BT\left(\frac{\partial^2}{\partial x_\alpha \partial x_\alpha}+\frac{\partial^2}{\partial x'_\alpha \partial x'_\alpha}\right)\sum_{i\neq j}\delta(\vec{x}-\vec{x}_i)\delta(\vec{x}'-\vec{x}_j), \quad (6)$$

and correspondingly for F_2,

$$\eta\frac{\partial F_2}{\partial t}=\frac{\partial}{\partial \vec{x}}\Bigg[F_2(t,\vec{x},\vec{x}')\left(\frac{\partial \mathcal{U}(\vec{x})}{\partial x}+\frac{\partial \mathcal{W}(\vec{x}-\vec{x}')}{\partial \vec{x}}-\vec{F}(t)\right)+\int d\vec{x}''F_3(t,\vec{x},\vec{x}',\vec{x}'')\frac{\partial \mathcal{W}(\vec{x}-\vec{x}'')}{\partial \vec{x}}\Bigg]$$
$$+\frac{\partial}{\partial \vec{x}'}\Bigg[F_2(t,\vec{x},\vec{x}')\left(\frac{\partial \mathcal{U}(\vec{x}')}{\partial \vec{x}'}+\frac{\partial \mathcal{W}(\vec{x}'-\vec{x})}{\partial \vec{x}'}-\vec{F}(t)\right)+\int d\vec{x}''F_3(t,\vec{x},\vec{x}',\vec{x}'')\frac{\partial \mathcal{W}(\vec{x}'-\vec{x}'')}{\partial \vec{x}'}\Bigg]$$
$$+k_BT\left(\frac{\partial^2}{\partial x_\alpha \partial x_\alpha}+\frac{\partial^2}{\partial x'_\alpha \partial x'_\alpha}\right)F_2(t,\vec{x},\vec{x}'). \quad (7)$$

The sets of Eqs. (5) and (7) are still insufficient to fully determine F_2, and therefore F_1, as now there appears the three-particle distribution function F_3, as well. Therefore, in analogy with Bogoliubov's hierarchy of the many-particle distribution function equations used in physical kinetics [17], only the entire set of N equations for $F_1,\ldots,F_N$ would be truly closed, but it would also be mathematically untractable.

Nevertheless, such a statistical approach provides a hierarchy of useful approximations, when the set of the first s equations is suitably truncated. The simplest mean-field approximation is obtained by replacing the pair distribution function $F_2(t,\vec{x},\vec{x}')$ with the product $F_1(t,\vec{x})F_1(t,\vec{x}')$ of the two corresponding one-particle distribution functions; hence we get the nonlinear integro-differential Fokker-Planck equation:

$$\eta\frac{\partial F_1(t,\vec{x})}{\partial t}=\frac{\partial}{\partial \vec{x}}\Bigg\{F_1(t,\vec{x})\Bigg[\frac{\partial}{\partial \vec{x}}\Bigg(\mathcal{U}(\vec{x})+\int d\vec{x}'\mathcal{W}(\vec{x}-\vec{x}')\times F_1(t,\vec{x}')\Bigg)-\vec{F}(t)\Bigg]+k_BT\frac{\partial F_1(t,\vec{x})}{\partial \vec{x}}\Bigg\}. \quad (8)$$

The physical interpretation of the last equation is that a particle at point $\vec{x}$ is affected by both the bare substrate potential $\mathcal{U}$ and an effective potential that reproduces its interaction with the $N-1$ surrounding particles—which are expected to be nonuniformly distributed in space. Thus, the total mean-field potential $\mathcal{U}^{\mathrm{mf}}$ reads

$$\mathcal{U}^{\mathrm{mf}}(\vec{x},t)=\mathcal{U}(\vec{x})+\int d\vec{x}'\mathcal{W}(\vec{x}-\vec{x}')F_1(t,\vec{x}'). \quad (9)$$

Note that the nonlocal Eq. (8) for F_1 is nonlinear. This may account for equilibrium and dynamical phase transitions (e.g., [18]) which are otherwise impossible to obtain through the standard linear Fokker-Planck equation [11,12].

B. Validity of the mean-field and local approximations

We discuss now the conditions under which we can introduce the mean-field approximation and/or ignore the nonlocality in the integro-differential Fokker-Planck equation (8). For simplicity we do this in the 1D case and for a periodic substrate potential $\mathcal{U}(x)=\mathcal{U}(x+l)$ with spatial period l.

In general, we can express the binary distribution function $F_2(x,x',t)$ as follows:

$$F_2(x,x',t)=F_1(x,t)F_1(x',t)G(x-x',x+x',t), \quad (10)$$

where the function G describes the statistical correlation between the two particles in the joint probability $F_2(x,x',t)$. The characteristic length scale of the one-particle distribution function $F_1(x,t)$ is of the order of l (l is the period of the potential energy). This can be seen in the equilibrium case with either weak or zero particle-particle interaction, where F_1 is a Boltzmann distribution, $F_1\propto\exp[-\mathcal{U}(x)/T]$. Also, this is easy to check for the particle distributions obtained in the following sections. On the other hand, for small particle densities $n\lambda\ll 1$ (n is the average particle density in 1D) and far from the condensation transition discussed below, the function G decreases on a length scale of the order of the interaction radius λ, where W is appreciably different from zero. Indeed, in this limit, G was estimated [12] to be $G\propto\exp[-W(x-x')/T]$. For higher particle densities $n\lambda\gg 1$, the average distance $a=1/n$ between particles becomes smaller than λ and the correlation between any two particles gets suppressed on length scales of about $a=1/n$. Therefore, we can assume that

$$G\approx 1 \text{ for } |x-x'|\gg \min\{n^{-1},\lambda\}. \quad (11)$$

Using Eq. (11) for $n\lambda\gg 1$, we obtain

$$\int dx'F_2(t,x,x')\frac{\partial \mathcal{W}(x-x')}{\partial x}$$
$$=F_1(t,x)\int dx'F_1(t,x')G(x-x')\frac{\partial \mathcal{W}(x-x')}{\partial \vec{x}}$$
$$\approx F_1(t,x)\int_{|x-x'|>a*}dx'F_1(t,x')\frac{\partial \mathcal{W}(x-x')}{\partial x}$$
$$\approx F_1(t,x)\int dx'F_1(t,x')\frac{\partial \mathcal{W}(x-x')}{\partial x}, \quad (12)$$

where $a*\sim a$. The third and fourth relations of Eq. (12) are evidently valid if $a\ll\lambda$. Thus, in this limit, Eq. (5) can be

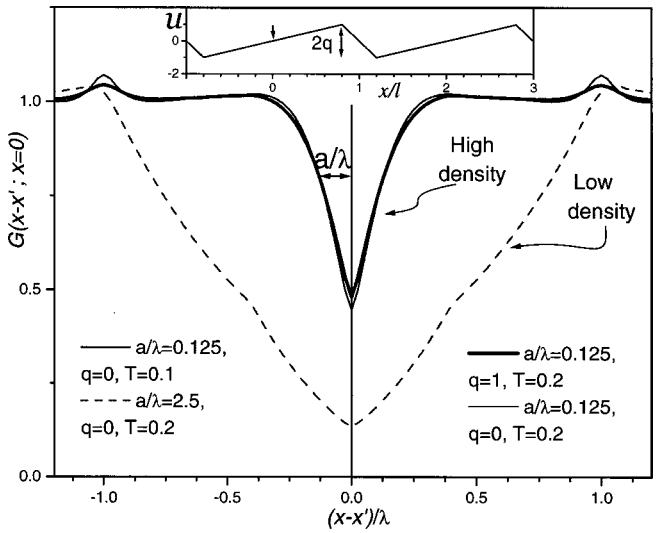

FIG. 1. (Color online) Deviation of the statistical correlation function G from its uncorrelated (mean-field) value $G=1$, versus distance $x-x'$ between particles, normalized by the interaction length λ. The interaction was taken as $W(x)=g(\lambda-|x|)/\lambda^2$, while the substrate potential $\mathcal{U}(x/l)$ is shown in the inset. The downward arrow in the inset marks the $x=0$ position where $G(x-x';x=0)$ was numerically computed. G substantially differs from 1 (its mean-field value) over distances $|x-x'|\sim a$, when the average distance $a=1/n$ between particles is much smaller than λ. In the opposite limit $a>\lambda$ (shown by the dashed line), we obtain $G<1$, on scales $|x-x'|<\lambda$. This result depends on neither temperature nor the substrate potential $\mathcal{U}$ in the range of parameters studied. Thus, we have numerically verified Eq. (11), which is used for the derivation of the mean-field approximation.

reduced to its mean-field form Eq. (8). Here, we assume that the contribution to the integral on the length scale of $1/n$ is negligible, which is correct for many families of interaction potentials [e.g., potentials that do not diverge at zero distance, $\partial\mathcal{W}(x=0)/\partial x=0$].

Thus, the assumption that $G\approx 1$ for $\lambda\gtrsim|x-x'|\gg a$ is the crucial one for the applicability of the mean-field approximation (see also [19]). This means that a particle interacts with many other particles resulting in averaging out the local fluctuations of individual particle-particle interactions. Even though $\lambda/a=n\lambda\gg 1$ is a standard condition for the validity of the mean-field approximation [20], we have performed numerical simulations of the Langevin equation (1) in order to obtain numerical evidence for Eq. (11). As we expected, Fig. 1 shows that G is significantly different from 1 in the region $|x-x'|\lesssim\lambda$ for low particle densities $n\lambda\ll 1$ (dashed curve in Fig. 1). In contrast to this, in the region $n\lambda\gg 1$, where the mean-field approximation is valid, the function G is close to 1 for $|x-x'|>a$ in Fig. 1. This important property does not strongly depend on the shape of the substrate potential and temperature. Thus, the contribution to the effective potential (9), associated with interparticle interactions, comes from the region $a<|x-x'|\lesssim\lambda$, where the approximation (11) is valid. This proves the applicability of the mean-field approximation.

In order to make the problem more tractable, we further discard nonlocal effects by assuming the scale λ of the interaction potential $\mathcal{W}(x-x')$ to be smaller than the scale l of the substrate potential $\mathcal{U}(x)$. This allows us to approximate the mean-field potential as follows:

$$\begin{aligned}\mathcal{U}^{\mathrm{mf}}(x,t) &= \mathcal{U}(x)+\int dx'\mathcal{W}(x-x')F_1(t,x')\\ &\approx \mathcal{U}(x)+F_1(t,x)\int dx'\mathcal{W}(x-x')\\ &= \mathcal{U}(x)+gF_1(t,x)\end{aligned}$$

with

$$g\equiv\int dx'\mathcal{W}(x-x'). \tag{13}$$

As a result, we obtain the partial differential equation

$$\eta\frac{\partial F_1}{\partial t}=\frac{\partial}{\partial x}\left[F_1\left(\frac{\partial\mathcal{U}}{\partial x}-F(t)\right)+k_BT(t)\frac{\partial F_1}{\partial x}+gF_1\frac{\partial F_1}{\partial x}\right], \tag{14}$$

which, in view of our previous discussion, is valid [11] when the average interparticle distance $a=1/n$ is much smaller than the particle interaction length λ, which, in turn, is much smaller than the unit cell period l of the substrate potential: i.e.,

$$a=n^{-1}\ll\lambda\ll l. \tag{15}$$

This mean-field equation (14) is analyzed in the forthcoming sections for both temperature and rocked ratchets.

Note that, if the inequality (15) regarding the particle-particle interaction is partly reversed, $\lambda\lesssim n^{-1}\ll l$, then Eq. (5) could still be handled in terms of Eq. (14) after introducing the effective interaction strength

$$g^{\mathrm{screened}}\equiv\int dx'\mathcal{W}(x-x')G(x-x',x+x') \tag{16}$$

to account for screening effects. Therefore, approximating g^{screened} to a spatial constant yields a qualitative description of the nonequilibrium behavior of the system even in parameter domains where the mean-field approximation is formally invalid.

III. COLLECTIVE MOTION OF LOCALLY INTERACTING PARTICLES IN A TEMPERATURE RATCHET

In this section we consider how local interparticle interactions influence the net current in a 1D ratchet system held out of equilibrium at a temperature that oscillates in time [3]. Note that this type of ratchet is a typical realization of the so-called Brownian or molecular motors where the directed motion is not related to any deterministic force [$F(t)=0$ in Eq. (14)]. This unusual net transport occurs via rectification of nonequilibrium fluctuations induced, e.g., by temperature oscillations $T(t)$. Note that temperature ratchets seem to be used by living organisms [21]: some microorganisms living in hot springs can extract energy out of regular thermal variations. In artificial devices thermal variations could be gener-

ated by electrical current oscillations via Joule's heating or via pressure oscillations [1].

The starting point of our analysis is the nonlinear Fokker-Planck equation for the sinusoidal temperature ratchet

$$\eta\frac{\partial F_1}{\partial t}=\frac{\partial}{\partial x}\left(F_1\frac{d\mathcal{U}}{dx}+k_BT(t)\frac{\partial F_1}{\partial x}+gF_1\frac{\partial F_1}{\partial x}\right), \tag{17}$$

with

$$T(t)=T(1+a\cos\omega t),\ a<1. \tag{18}$$

For convenience, hereafter T denotes the average temperature, i.e.,

$$T\equiv\frac{\omega}{2\pi}\int_0^{2\pi/\omega}T(t)dt.$$

In the general case, an analytical study of Eq. (17) is too complicated. However, if the period of the temperature oscillations $2\pi/\omega$ is much shorter than the other characteristic time scales in the problem, then the particles cannot adjust to the varying temperature, but rather experience an average effect due to the temperature oscillations. Thus, it is reasonable to expect that the system relaxes close to the equilibrium state corresponding to the average temperature T. This equilibrium solution

$$F_1(x,a=0)\equiv\phi_0=\phi_0(x) \tag{19}$$

satisfies the nonlinear equation

$$\mathcal{U}'(x)\phi_0+g\phi_0\frac{d\phi_0}{dx}+k_BT\frac{d\phi_0}{dx}=0, \tag{20}$$

which can be solved in implicit form,

$$C(n)\exp\left(-\frac{\mathcal{U}(x)}{k_BT}\right)=\phi_0(x)\exp\left(\frac{g}{k_BT}\phi_0(x)\right)\equiv Z(\phi_0), \tag{21}$$

where the constant $C(n)$ is determined by the normalization condition

$$\int_0^l dx\ \phi_0(x)=nl,$$

where n is the particle density and l is the substrate unit cell. The equilibrium distribution ϕ_0 coincides with the usual Boltzmann distribution if the particle interaction is switched off, $g=0$. In Appendix A, we study Eq. (20) in the presence of nonlocal interactions.

A. Condensation

Here, one can see how *nonlinearity produces a phase transition*. Equation (21) always admits a solution if the particles repel each other, $g>0$ (see Fig. 2, inset). However, in the case of attracting particles, $g<0$, the transcendental Eq. (21) has a solution only if (see Fig. 2)

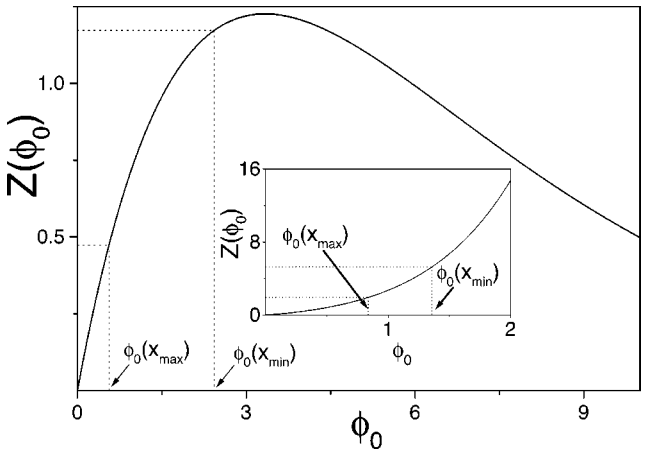

FIG. 2. Graphical solution of the transcendental equation (21) for a subcritical density of attracting particles. With increasing density of the particles, both values $\phi_0(x_{\min})$ and $\phi_0(x_{\max})$ increase. Horizontal dotted lines represent $Z(\phi_0)=Z(\phi_0(x_{\min}))=Ce^{-\mathcal{U}^{\min}/k_BT}$ (upper) and $Z(\phi_0)=Z(\phi_0(x_{\max}))=Ce^{-\mathcal{U}^{\max}/k_BT}$ (lower), respectively. As soon as $Z(\phi_0(x_{\min}))$ reaches the maximum value $\max[Z(\phi_0)]=k_BT/e|g|$, the transcendental equation admits no solution and a phase transition occurs. Note that the decreasing $Z(\phi_0)$ branch is unstable. As shown in the inset, one can always find the solution to Eq. (21) for repelling particles since $Z(\phi_0)$ is a monotonic increasing function of ϕ_0. We used $|g|/k_BT=\pm0.3$ to plot the function $Z(\phi_0)$.

$$C(n)\exp\left(-\frac{\min[\mathcal{U}(x)]}{k_BT}\right)<\frac{k_BT}{e|g|}.$$

Here, e is Euler's number (2.71…). Indeed, the functional $Z(\phi_0)$ computed at the minimum $x_{\min}$ of $\mathcal{U}(x)$, $Z(\phi_0(x_{\min}))$, approaches its maximum value

$$\max_{\phi_0}Z(\phi_0)=\frac{k_BT}{e|g|}$$

as the particle density increases. In other words, more and more particles accumulate near $x_{\min}$, which in turn attract additional particles from even further away. Eventually, the particle attraction wins over the random thermal noise. This occurs at a critical value $n_{\rm crit}$ of the particle density when $Z(\phi_0(x_{\min}))$ equals the maximum value $Z(\phi_0)=k_BT/e|g|$. At higher densities the equilibrium distribution (21) cannot be sustained any longer; thermal noise cannot prevent the *condensation* of a finite fraction of the nonideal (interacting) gas particles into the liquidlike phase at the bottom of the potential wells. Therefore, the analysis presented below is not valid for $n>n_{\rm crit}$. Note that such a phase transition is not related to the nonequilibrium condition of the system; more exciting dynamical phase transitions due to the interplay of nonequilibrium and nonlinearity will be revealed by solving the Fokker-Planck equation (17).

B. Effective potentials

The equation for the perturbation correction $\psi=\psi(x)\equiv F_1-\phi_0$ from the equilibrium state ϕ_0 is

$$\frac{\partial \psi}{\partial \tau} = \frac{1}{\eta\omega}\frac{\partial}{\partial x}\left(\psi\frac{d\mathcal{U}^{\text{eff}}}{dx} + g\psi\frac{\partial \psi}{\partial x} + [k_B T^{\text{eff}}(x) + k_B T a(\cos\tau)]\frac{\partial \psi}{\partial x}\right) + \frac{k_B T a}{\eta\omega}\cos\tau\left(\frac{d^2\phi_0}{dx^2}\right), \quad (22)$$

where $\tau \equiv \omega t$ is the dimensionless time, while the effective potential and temperature are defined as

$$\mathcal{U}^{\text{eff}}(x) = \mathcal{U}(x) + g\phi_0, \quad (23)$$

$$k_B T^{\text{eff}}(x) = k_B T + g\phi_0. \quad (24)$$

These equations can be qualitatively interpreted if we separate the running particles, a relatively small fraction of about $|\psi(x)|/\phi_0(x)$ at the point x, from those trapped at the substrate minima. The moving particles experience the potential $\mathcal{U}^{\text{eff}}$ generated by both the substrate and the trapped particles.

In the case of *repulsive* particle interaction, such an effective potential is smoother than the bare substrate potential (see Fig. 3) because the particles occupying the bottom of the potential wells tend to repel the running particles away from the potential minima.

In contrast to this, with increasing density of *attracting* particles, the wells of the effective potential grow even deeper than the substrate wells (Fig. 4). Note that the particle-particle interaction also induces a spatial dependence of the effective temperature, which implies a spatial dependence of the diffusion constant of the running particles. The effective temperature and potential exhibit the same asymmetry for the case of attracting particles, meaning that the positions of their maxima and minima coincide. In this respect, we say that *for repelling particles the effective temperature and the effective potential have opposite asymmetry*.

C. Perturbative approach

Next we develop a perturbation approach to study the time dependence of Eq. (22) in analogy with the extensively studied case of noninteracting particles [1,22]. In the high-frequency limit, the solution for ψ can be expanded in powers of the reciprocal of temperature frequency as

$$\psi = \sum_{i=1}^{\infty} \frac{1}{(\eta\omega)^i}\phi_i(\tau, x, a) \quad (25)$$

with the periodic conditions $\phi_i(\tau + 2\pi, x) = \phi_i(\tau, x) = \phi_i(\tau, x + l)$ and normalization $\int_0^l dx\, \phi_{i\neq 0}(x) = 0$. Substituting Eq. (25) into Eq. (22) and collecting all terms with the same power of $1/\omega$, we iteratively derive the set of equations (hereafter we define $' \equiv d/dx$)

$$\frac{\partial \phi_1}{\partial \tau} = k_B T a(\cos\tau)\phi_0'',$$

$$\frac{\partial \phi_2}{\partial \tau} = \frac{\partial}{\partial x}\left((\mathcal{U}^{\text{eff}})'\phi_1 + (k_B T^{\text{eff}} + k_B T a\cos\tau)\frac{\partial \phi_1}{\partial x}\right),$$

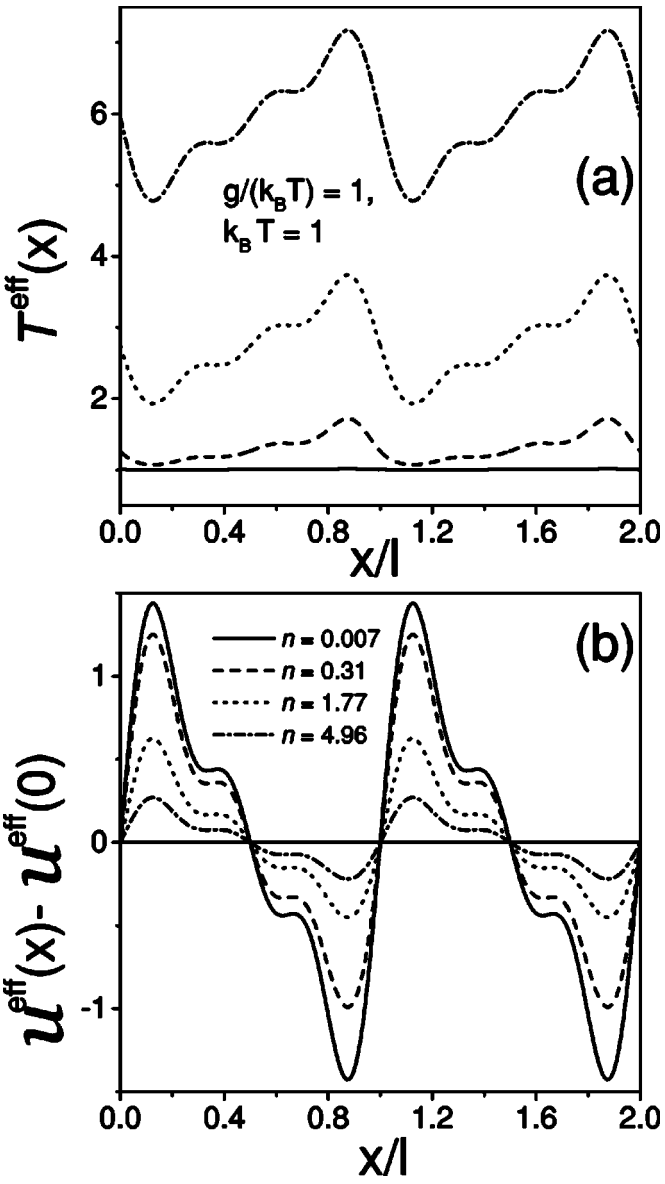

FIG. 3. (a) The spatial dependence of the effective temperature T^{eff} and (b) the effective potential $\mathcal{U}^{\text{eff}} - \mathcal{U}^{\text{eff}}(0)$ for repelling particles and for different values of their density n. Both the effective temperature T^{eff} and the effective potential energy $\mathcal{U}^{\text{eff}}$ are shown in arbitrary units. The bare substrate potential is chosen as $\mathcal{U}(x) = \mathcal{U}^{\text{ramp}}(x) \equiv \sin(2\pi x/l) + (1/2)\sin(4\pi x/l) + (1/3)\sin(6\pi x/l)$. Mutual repulsion of particles out of the potential wells causes the flattening the "effective" potential with increasing n. The positions of the maxima of $\mathcal{U}^{\text{eff}}(x)$ coincide with the minima of $T^{\text{eff}}(x)$, and vice versa. This indicates that $T^{\text{eff}}(x)$ and $\mathcal{U}^{\text{eff}}(x)$ have opposite asymmetry.

$$\frac{\partial \phi_3}{\partial \tau} = \frac{\partial}{\partial x}\left((\mathcal{U}^{\text{eff}})'\phi_2 + (k_B T^{\text{eff}} + k_B T a\cos\tau)\frac{\partial \phi_2}{\partial x} + g\phi_1\frac{\partial \phi_1}{\partial x}\right)$$

$$\vdots \quad (26)$$

Thus, we obtain an infinite set of equations having the form

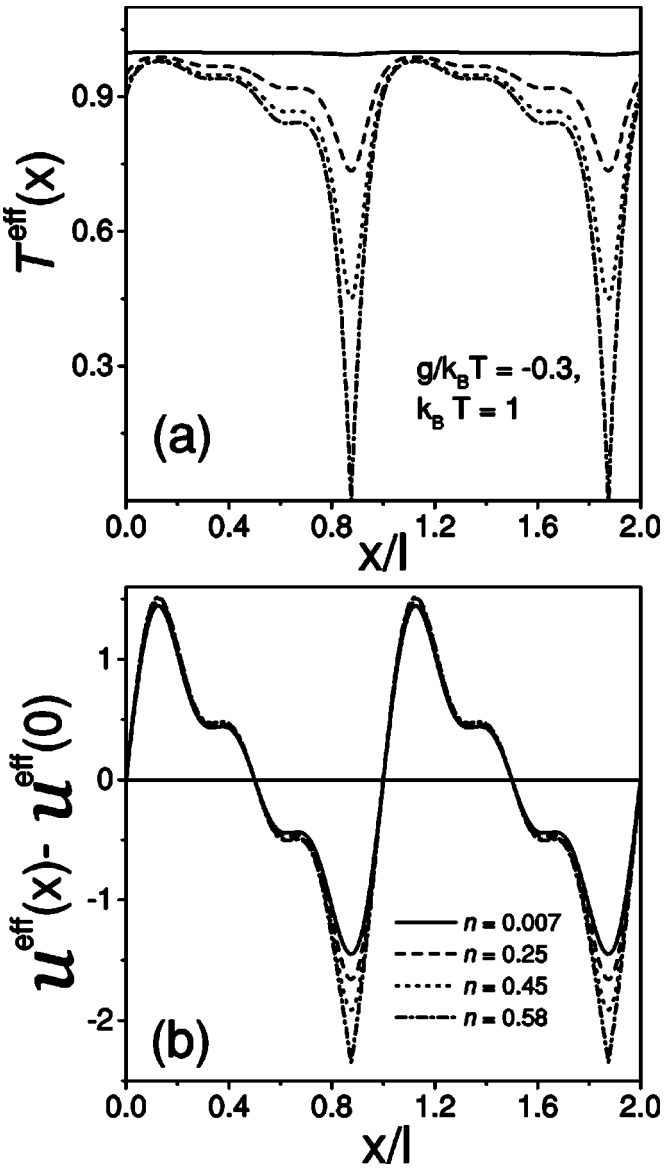

FIG. 4. Same as in Fig. 3, but for attracting particles. The "effective" potential wells deepen due to particle clustering around its minima. The effective temperature T^{eff} has a maximum where $\mathcal{U}^{\mathrm{eff}}$ has a maximum, and vice versa. The condensation of the attracting particles in the potential minima $x=x_{\min}$ occurs as $T^{\mathrm{eff}}(x_{\min})$ drops to zero.

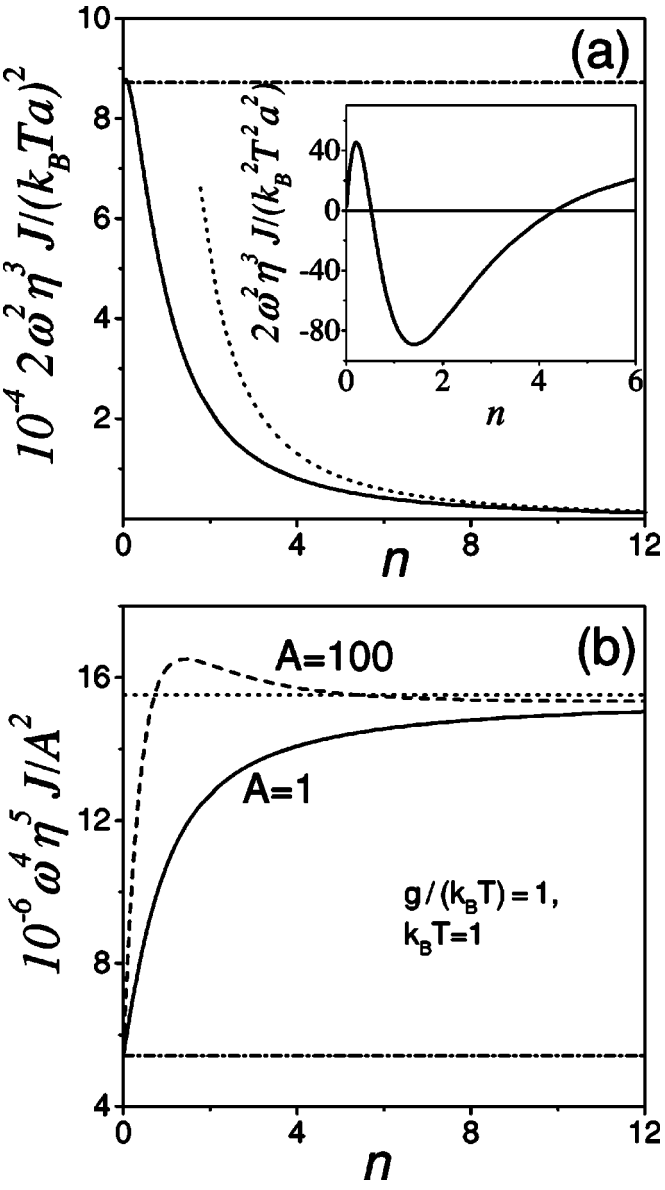

FIG. 5. Net velocity V_{dc} versus density n of repelling particles for temperature (a) and rocked ratchets (b) with the substrate potential $\mathcal{U}(x)=\mathcal{U}^{\mathrm{ramp}}(x)$ defined in Fig. 3. The dash-dotted lines correspond to the case of noninteracting particles, while the dotted lines show the high-density limits. The inset in (a) shows the case of two current inversions with increasing particle density for the temperature ratchet with $\mathcal{U}(x)=\sin(2\pi x/l)+0.2\sin(4\pi x/l-0.45)-0.06\sin(6\pi x/l-0.45)$.

$$\frac{\partial\phi_i}{\partial\tau} = \Psi(\tau, \phi_0, \ldots, \phi_{i-1}). \tag{27}$$

The solution of the ith such equation can be written, also by iteration, as

$$\phi_i = \int_0^\tau d\tilde{\tau}\, \Psi(\tilde{\tau}, \phi_0(\tilde{\tau}), \ldots, \phi_{i-1}(\tilde{\tau})) + P_i(x). \tag{28}$$

This means that at the ith step ϕ_i is determined, apart from a still unknown periodic function $P_i(x)$. The function P_i can be found at the $(i+1)$th step by imposing simultaneously the time periodicity of ϕ_{i+1}, the spatial periodicity of P_i, and the normalization of ϕ_i.

The frequency range where our perturbation technique applies can be estimated from the convergence condition

$$\frac{|\phi_{i+1}|}{\eta\omega|\phi_i|} \ll 1$$

of expansion (25). In view of Eq. (26) we get

$$\omega \gg \omega_c = \frac{1}{\eta l^2} \max\{\Delta \mathcal{U}^{\text{eff}}, k_B T^{\text{eff}}(x)\}, \tag{29}$$

where

$$\Delta \mathcal{U}^{\text{eff}} = \max[\mathcal{U}^{\text{eff}}(x)] - \min[\mathcal{U}^{\text{eff}}(x)].$$

Moreover, there is one more restriction on the validity of our perturbation scheme, namely, $|\phi_1| \ll \phi_0$, or equivalently

$$a \ll \eta\omega \frac{l^2 \min[T^{\text{eff}}(x)]}{T \Delta \mathcal{U}^{\text{eff}}}. \tag{30}$$

This constraint on a follows from the tendency of the system to be close to equilibrium and, therefore, rules out large temperature oscillations.

D. Net currents

The detailed calculations for the perturbation scheme outlined above are presented in Appendix B. Here we only report our final result for the net particle current:

$$J(n,\omega,T) = \frac{k_B^2 T^2 a^2}{2\omega^2 \eta^3 \left(\int_0^l dx/\phi_0 \right)} \int_0^l dx \left(\frac{(\mathcal{U}'')^2 \mathcal{U}' (4k_B T + 5g\phi_0)}{(k_B T + g\phi_0)^3} - \frac{2k_B T (\mathcal{U}')^3 \mathcal{U}'' (4k_B T + 5g\phi_0)}{(k_B T + g\phi_0)^5} - \frac{g\phi_0 (\mathcal{U}')^5}{(k_B T + g\phi_0)^7} (6k_B^2 T^2 + 10 g k_B T \phi_0 + 3g^2 \phi_0^2) \right). \tag{31}$$

In the case of noninteracting particles, $g=0$, the expression (31) coincides with earlier predictions—see Eq. (2.58) in [1] for $T(t)=T[1+a\cos(\omega t)]$. Moreover, the general behavior of the net current is quite robust with respect to changing the time dependence of the temperature; for instance, Eq. (4.5) of Ref. [23], obtained for $T(t)=T[1+a\sin(\omega t)]^2$ and $g=0$, differs from Eq. (31) by a mere multiplicative factor of 4.

Now, the behavior of the rectified current (31) can be studied for low and high particle densities. In the limit $n \to 0$, Eq. (21) can be solved as

$$\phi_0 = C \exp\left(-\frac{\mathcal{U}(x)}{k_B T} \right) \left[1 - \frac{gC}{k_B T} \exp\left(-\frac{\mathcal{U}(x)}{k_B T} \right) \right] + O(C^3), \tag{32}$$

where C is related to the particle density by

$$C(n) = \frac{nl}{\Pi_{-1}} + \frac{g n^2 l^2 \Pi_{-2}}{k_B T (\Pi_{-1})^3} + O(n^3). \tag{33}$$

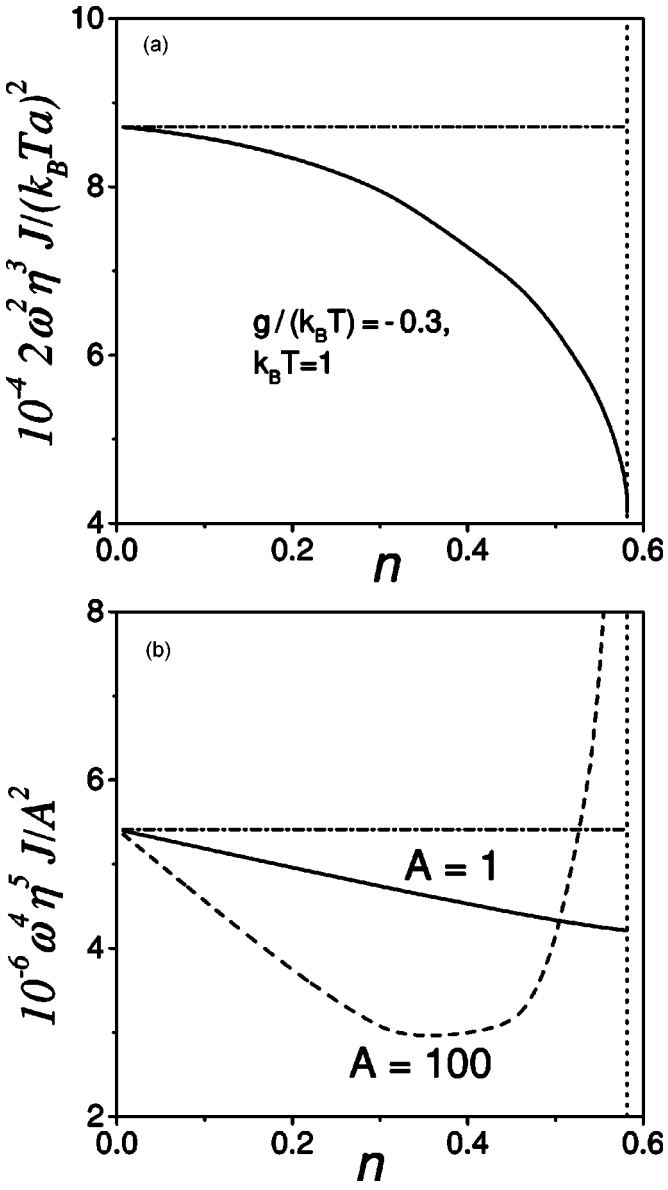

FIG. 6. Net average velocity V_{dc} versus density n of attracting particles. Notation is as in Fig. 5 with the same substrate potential $\mathcal{U}(x)=\mathcal{U}^{\text{ramp}}(x)$ used in Fig. 3: (a) temperature ratchet; (b) rocked ratchet. Here, the vertical dotted lines mark the critical particle density n_{crit} where the condensation takes place.

Here we introduce the notation

$$\Pi_m \equiv \int_0^l dx \exp(m\mathcal{U}/k_B T). \tag{34}$$

Combining Eqs. (31) and (33) yields

$$J(n \to 0) = J_1 n + (J_2 - J_3) n^2 + O(n^3), \tag{35}$$

where

$$J_1 = \frac{2a^2 l \int_0^l dx\, \mathcal{U}' (\mathcal{U}'')^2}{\omega^2 \eta^3 \Pi_1 \Pi_{-1}}, \tag{36}$$

$$J_2 = \frac{2a^2 g l^2 \int_0^l dx\, \mathcal{U}'(\mathcal{U}'')^2(\Pi_{-2}\Pi_1 - l\Pi_{-1})}{\omega^2 \eta^3 k_B T(\Pi_1)^2(\Pi_{-1})^3}, \tag{37}$$

$$J_3 = \frac{a^2 n^2 l^2 g \int_0^l dx \exp(-\mathcal{U}/k_B T)[6(\mathcal{U}')^5/(k_B^2 T^2) + 7\mathcal{U}'(\mathcal{U}'')^2 - 30\mathcal{U}''(\mathcal{U}')^3/k_B T]}{2k_B T\omega^2 \eta^3 \Pi_1(\Pi_{-1})^2}. \tag{38}$$

The current J_1 is not related to interaction and was earlier obtained by Reimann [1]. In contrast, the currents J_2 and J_3 are caused by the interparticle interaction and vanish for $g \to 0$.

If $\int_0^l dx\, \mathcal{U}'(\mathcal{U}'')^2$ is close to zero, we expect that current inversions may occur with increasing particle density n. To this purpose we must tune the potential $\mathcal{U}$ so that the terms of Eq. (38) proportional to n and n^2 have opposite signs [see inset of Fig. 5(a)].

Next let us consider the high-density limit $n \to \infty$. The solution of Eq. (21) simplifies to

$$\phi_0 = n - \frac{\mathcal{U}(x)}{g} + O(1/n) \tag{39}$$

with the assumption $\int_0^l \mathcal{U}(x)dx = 0$, for an appropriate offset of $\mathcal{U}(x)$. In the first approximation in $1/n$ we obtain

$$J(n \to \infty) = \frac{5k_B^2 T^2 a^2}{2\omega^2 \eta^3 g^2 l} \frac{1}{n} \int_0^l dx\, \mathcal{U}'(\mathcal{U}'')^2 + O\left(\frac{1}{n^2}\right). \tag{40}$$

Note that the sign of the current is the same in the limits $n \to 0$ and $n \to \infty$ and is defined by the sign of the integral $\int_0^l dx\, \mathcal{U}'(\mathcal{U}'')^2$.

As shown in Fig. 5(a), the net velocity $V_{dc} = J/n$ typically decays rapidly with increasing density of the repelling particles. Such an effect can be easily interpreted considering the dependence of the effective potential on n. Indeed, since the repelling particles tend to expel each other from the potential wells, the effective potential $\mathcal{U}^{\text{eff}}$ flattens out and this suppresses the ratchet asymmetry (Fig. 3).

In the case of attracting particles, the situation is more complicated because our perturbation approach loses its validity when the particle density approaches the critical value n_{crit} corresponding to the equilibrium particle condensation. However, for a ratchet substrate the net particle velocity decays with n [see Fig. 6(a)], no matter what the sign of g, in the region where the perturbation technique is applicable.

IV. COLLECTIVE MOTION OF LOCALLY INTERACTING PARTICLES IN A ROCKED RATCHET

In this section we study a class of ac driven ratchets commonly used, for instance, to rectify the vortex motion in superconductors with artificially tailored asymmetric pinning potential [8]. A gas of interacting particles in such rocked ratchets is approximately described by the equation

$$\frac{\partial F_1}{\partial t} = \frac{\partial}{\partial x}\left((\mathcal{U}' - A\sin\omega t)F_1 + k_B T\frac{\partial F_1}{\partial x} + gF_1\frac{\partial F_1}{\partial x}\right). \tag{41}$$

In analogy with the previous section, we introduce the ansatz $F_1 = \phi_0 + \psi$ for the solution of Eq. (41). Here, the equilibrium particle distribution ϕ_0 is defined by Eq. (21) and the perturbation ψ obeys the equation

$$\eta\frac{\partial \psi}{\partial t} = \frac{\partial}{\partial x}\left(\psi[(\mathcal{U}^{\text{eff}})' - A\sin\omega t] + g\psi\frac{\partial \psi}{\partial x} + k_B T^{\text{eff}}(x)\frac{\partial \psi}{\partial x}\right) - A(\sin\omega t)\phi_0', \tag{42}$$

with effective potential $\mathcal{U}^{\text{eff}}$ and temperature T^{eff} defined in Eq. (24). In the high-frequency limit $\omega \to \infty$, one can iteratively approximate ψ by computing the expansion (25) term by term. Such a perturbation approach is valid if condition (29) for the drive frequency is satisfied and the drive amplitude is restricted to sufficiently small values, that is,

$$A \ll \eta\omega\frac{lk_B \min[T^{\text{eff}}(x)]}{\Delta\mathcal{U}^{\text{eff}}}. \tag{43}$$

In order to calculate the net ratchet current in leading order, all terms of the expansion (25) up to the fifth order must be retained. Skipping cumbersome algebraic passages (along the line of Appendix B), one arrives at the final result

$$J^{\text{rocked}} = \frac{A^2}{\omega^4 \eta^5\left(\int_0^l dx/\phi_0\right)}(j_{41} + A^2 j_{42}), \tag{44}$$

with

$$j_{41} = \int_0^l dx\, \mathcal{U}'(\mathcal{U}''')^2\left(1 + \frac{g\phi_0}{2(k_B T + g\phi_0)}\right),$$

$$j_{42} = \int_0^l dx \left(\frac{g\phi_0 \mathcal{U}'(\mathcal{U}'')^2}{8(k_B T + g\phi_0)^3} - \frac{g\phi_0 (\mathcal{U}')^5 (k_B^2 T^2 - 8g\phi_0 k_B T + 6g^2 \phi_0^2)}{64(k_B T + g\phi_0)^7} + \frac{g\phi_0 \mathcal{U}' k_B^2 T^2}{2d^4 (k_B T + g\phi_0)^3} \right). \quad (45)$$

Here, d denotes the effective distance

$$d^2 = \frac{4\int_0^l dx[\phi_0/(k_B T + g\phi_0)]}{\int_0^l dx[(\mathcal{U}')^2 \phi_0/(k_B T + g\phi_0)^3]}. \quad (46)$$

Qualitative interpretation

In contrast with the temperature ratchet, the net velocity through the ac ratchet increases with increasing density n of the repelling particles [see Fig. 5(b)], with asymptotic behavior

$$j_{41}(n \to \infty) \approx 1.5 j_{41}(n \to 0). \quad (47)$$

In order to understand the physical origin of such behavior, we recall that the effective potential acting on moving particles flattens with increasing density of the repelling particles.

This mechanism is illustrated schematically in Fig. 7(a) where a typical effective potential at low (solid curve) and high density (dotted curve) is drawn for the sake of clarity. If the temperature and the amplitude of the ac force are low enough, a running particle cannot overcome the potential barriers for low particle density [solid curve, Fig. 7(b)]. Therefore, the particle (solid circle) remains trapped in a potential minimum during the ac tilting of the potential [in Fig. 7(b), the upper and lower panels show the effective potential subject to maximum tilt both to the right and to the left]. Thus, the current has to be very small.

However, the particle can overcome the lower potential barriers of the effective potential corresponding to *higher* particle density (dotted curve), when the potential is tilted [Fig. 7(b), a particle (open circle) can move to the left]. The above behavior leads to the "activation" of the net motion for higher n. Thus, the dc net current is obviously enhanced with increasing density of particles for small enough amplitude A of the ac force.

On the other hand, if A is strong enough, particles can easily pass through the potential barriers in the preferable direction even for low particle density when the potential is tilted [Fig. 7(c), upper panel, solid curve]. In such a case, a particle (solid circle) moves easily to the left, while barriers prevent the motion in the opposite direction [Fig. 7(c), lower panel], resulting in an effective rectification. The suppression of the barriers (associated with increasing the density n of repelling particles) stimulates the undesirable motion in the direction which is opposite to the net current [Fig. 7(c), lower panel, dotted curve]. With increasing A, this has to

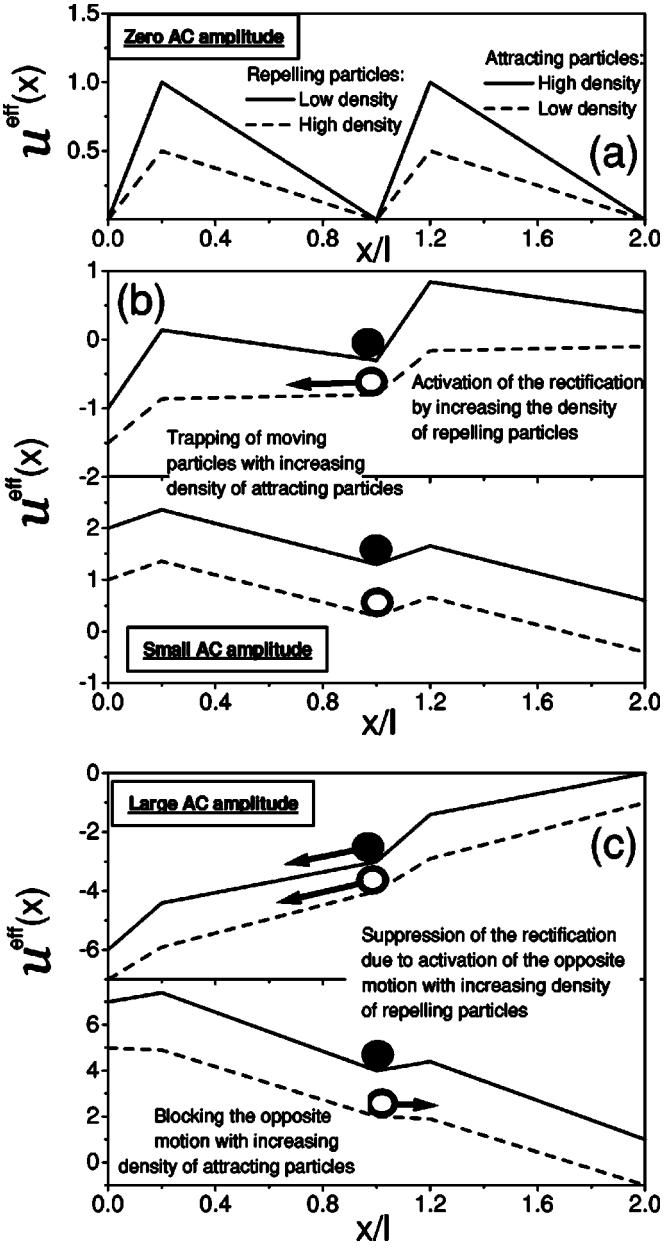

FIG. 7. Schematics of the n dependence of V_{dc} for a rocked ratchet. (a) The original potential (solid line) and flatter effective potential (dashed line) due to repelling interaction among particles. (b) The small amplitude of the ac force, which tilts the effective potential from $\mathcal{U}^{eff} - Ax$ (upper panel) to $\mathcal{U}^{eff} + Ax$ (lower panel), could not produce a net motion in the bare potential (solid line) at low temperatures because of the potential barriers. However, the suppressed barriers (dashed line) for a high density of repelling particles can be overcome resulting in directed particle motion. (c) At large amplitudes, the ac particle motion in the bare potential gets rectified as the tilt is strong enough. Indeed, a particle (solid circle) moves easily only when the potential is tilted to $\mathcal{U}^{eff} - Ax$ [upper panel in (c)]; the suppression of the barriers also activates a substantial particle flow in the opposite direction, thus reducing the ratchet rectification power. For the attracting particles, the effective potential deepens with increasing n. The dependence of V_{dc} on n for attracting particles is discussed in the text.

result in a change of the dependence of V_{dc} on the particle density, i.e., from an increasing to a decreasing function of n. This is consistent with our calculations: V_{dc} contains terms proportional to both A^2 and A^4, which are responsible for the change of the dependence of the net velocity on the particle density [Fig. 5(b), solid and dashed curves].

For attracting particles, the potential wells deepen with increasing particle density. In Fig. 7 this corresponds to the modification of the effective potential $\mathcal{U}^{\text{eff}}$ from a dashed (low density) to a solid (high density) profile. Thus, particles (open circle), moving on the bare potential (low-density case), get trapped by the deeper potential wells at higher density [Fig. 7(b), solid circle, solid curve]; at small A, the net velocity diminishes in the case of attracting particles. This is consistent with the results displayed in Fig. 6(b), solid line; namely, the net velocity for the attracting particles decays linearly with n for low values of A, practically up to $n=n_{\text{crit}}$. This behavior is associated with the n dependence of $j_{41}(n)$. At larger ac amplitudes, the growing potential barrier stops the undesirable motion in the opposite direction with respect to the net transport [Fig. 7(c), lower panel]. This enhances the rectification as seen in Fig. 6, dashed line. In other words, with increasing A the term proportional to A^4 becomes important, thus resulting in the strong enhancement of the net velocity for $n \to n_{\text{crit}}$, as now the deepening wells provide a more pronounced anisotropy in the system.

V. CONCLUSIONS

We have developed a perturbation scheme to study an open system of interacting particles diffusing on an asymmetric substrate. The net velocity V_{dc} of locally interacting particles maintained out of equilibrium by temperature oscillations or external ac drives has been analyzed as a function of the particle density in the high-frequency limit. We have shown that V_{dc} diminishes with increasing density of the repelling particles in a temperature ratchet, while it grows in a rocked ratchet.

Our perturbation scheme is applicable to a system of attracting particles, too, but for densities below a critical value n_{crit}, when the nonideal gas of interacting particles begins to condense at the bottom of the potential wells. In this case V_{dc} decays with increasing density n of the attracting particles at small drive amplitudes A, while it may shoot up at large enough drive amplitudes. The dependence of V_{dc} on the particle density n has been related to the deepening of the potential wells for attracting particles and to their smoothing for repelling particles. The net flow of one (or more) species of interacting particles in a periodic ratchet can thus be controlled by varying their density.

The unusual dynamics observed in this system can be understood in terms of the flattening of the asymmetric effective potential acting on the repelling particles and the deepening of the effective potential wells binding the attracting particles. These very different mechanisms suggest an efficient control of the ratchet rectification process by tuning the density of the interacting particles.

ACKNOWLEDGMENTS

This work was supported in part by the National Security Agency (NSA) and Advanced Research and Development Activity (ARDA) under Air Force Office of Scientific Research (AFOSR) Contract No. F49620-02-1-0334; and also by the U.S. National Science Foundation Grant No. EIA-0130383.

APPENDIX A: NONLOCAL INTERACTION: THERMODYNAMIC ANALOGIES

It is interesting to note that in the general nonlocal case the equilibrium solution ϕ_0 satisfies Eq. (8)

$$C(n)\exp\left(-\frac{\mathcal{U}}{k_BT}\right) = \phi_0 \exp\left(\frac{1}{k_BT}\int_{-\infty}^{\infty} dx'\,\phi_0(x')\mathcal{W}(x-x')\right)$$

or, equivalently, using the "free energy" $\mathcal{F}_0(x)$,

$$\mathcal{F}_0(x) = \mathcal{U}(x) + \int_{-\infty}^{\infty} dx'\mathcal{W}(x-x')\exp\left(-\frac{\mathcal{F}_0(x')}{k_BT}\right) - k_BT\ln C(n), \tag{A1}$$

with

$$\phi_0(x) = \exp\left(-\frac{\mathcal{F}_0(x)}{k_BT}\right).$$

Introducing the "effective entropy" $\mathcal{S}(x)$ through the identity

$$\phi_0(x) = C(n)\exp\left(-\frac{\mathcal{U}(x) - k_BT\mathcal{S}(x)}{k_BT}\right),$$

Eq. (A1) for $\mathcal{F}_0(x)$ can be rewritten as

$$\mathcal{S}(x) = -\frac{C(n)}{k_BT}\int_{-\infty}^{+\infty} dx' e^{\mathcal{S}(x')}e^{-\mathcal{U}(x')/k_BT}\mathcal{W}(x-x') = -\frac{C(n)}{k_BT}\int_{-\infty}^{\infty} dx' e^{\mathcal{S}(x-x')}e^{-\mathcal{U}(x-x')/k_BT}\mathcal{W}(x'). \tag{A2}$$

Equations (A1) and (A2) for the effective free energy and the entropy are nonlinear and nonlocal because of the particle interactions. Note that the effective free energy $\mathcal{F}_0(x)$ and entropy $\mathcal{S}(x)$ satisfy the usual thermodynamic relation

$$\mathcal{F}_0(x) = \mathcal{U}(x) - k_BT\mathcal{S}(x).$$

APPENDIX B: TEMPERATURE RATCHET: A HIGH-FREQUENCY EXPANSION

In this appendix, we show how our iterative procedure for calculating the one-particle distribution function F_1 and the probability current J can be carried out for a temperature ratchet in the high-frequency limit. Integrating the first equation of set (26), for the distribution function in the first approximation we get

$$\phi_1 = k_BTa(\sin\tau)\phi_0'' + P_1(x),$$

where the still unknown periodic function $P_1(x)$ is normalized to zero, $\int_0^l dx\, P_1 = 0$. Substituting this equation for ϕ_1 into the second equation of set (26) yields an equation for the second coefficient of expansion (25), namely,

$$\frac{\partial \phi_2}{\partial \tau} = \frac{\partial}{\partial x}\{k_B T a(\sin\tau)\phi_0''(\mathcal{U}^{\rm eff})' + [k_B T^{\rm eff}(x) + k_B T a\cos\tau]k_B T a(\sin\tau)\phi_0'''\} + \frac{d}{dx}[P_1(\mathcal{U}^{\rm eff})' + k_B T^{\rm eff}P_1'] + k_B T a(\cos\tau)P_1''.$$

The right-hand side of the last equation must contain only zero-mean time-oscillating terms, lest the function ϕ_2 increases with time and eventually exceed $\eta\omega\phi_1$ and $\eta^2\omega^2\phi_0$, thus breaking the perturbation scheme. Setting to zero the secular terms leads to an equation for P_1,

$$P_1(\mathcal{U}^{\rm eff})' + k_B T^{\rm eff}P_1' = -j_1,$$

with the integration constant j_1 being a probability current. Taking P_1 as $P_1(x)=B(x)\phi_0(x)/(k_BT+g\phi_0)$, we obtain $B'=j_1/\phi_0>0$. Now, if $j_1\neq 0$, then B monotonically increases and the function $P_1(x)$ becomes aperiodic in space. This conflicts with the condition of spatial periodicity of P_2. Therefore, we come to the conclusion that $j_1=0$, i.e., $B=$const. Moreover, the function $P_1(x)=B\phi_0(x)/[k_BT+g\phi_0(x)]$ satisfies the condition $\int_0^l dx\, P_1=0$ only if we take $P_1(x)\equiv 0$. As a result, the equation for ϕ_2 (with P_1 identically zero) takes the form

$$\frac{\partial \phi_2}{\partial \tau} = k_B T a(\sin\tau)\frac{d}{dx}[\phi_0''(\mathcal{U}^{\rm eff})' + k_B T^{\rm eff}\phi_0'''] + \frac{1}{2}k_B^2T^2a^2(\sin 2\tau)\phi_0'''. \tag{B1}$$

Integrating the last equation over τ yields the following expression for ϕ_2:

$$\phi_2 = -k_B T a(\cos\tau)\frac{d}{dx}[\phi_0''(\mathcal{U}^{\rm eff})' + k_B T^{\rm eff}\phi_0'''] - \frac{1}{4}k_B^2T^2a^2(\cos 2\tau)\phi_0''' + P_2. \tag{B2}$$

The time-independent spatially periodic function P_2 and the probability current $J_2=j_2/\omega^2\eta^3$ can be obtained only by working out the equation for ϕ_3, i.e., retaining all the terms up to order $1/\omega^2$:

$$\frac{\partial \phi_3}{\partial \tau} = \frac{\partial}{\partial x}\Bigg[\Bigg(-k_B T a\cos\tau[\phi_0''(\mathcal{U}^{\rm eff})' + k_B T^{\rm eff}\phi_0''']' - \frac{1}{4}k_B^2T^2a^2\cos 2\tau\phi_0''' + P_2\Bigg)(\mathcal{U}^{\rm eff})' + k_B(T^{\rm eff} + Ta\cos\tau)\frac{\partial}{\partial x}\Bigg(-k_B T a\cos\tau[\phi_0''(\mathcal{U}^{\rm eff})' + k_B T^{\rm eff}\phi_0''']' - \frac{1}{4}k_B^2T^2a^2\cos 2\tau\phi_0''' + P_2\Bigg) + gk_B^2T^2a^2\sin^2\tau\phi_0''\phi_0'''\Bigg].$$

Integrating the equation above with $P_2=0$ would generate undesirable aperiodic terms which increase linearly with time. Therefore, we must determine an appropriate function P_2 in order to avoid breaking our perturbation scheme. We start deriving an equation for P_2 of the form

$$\frac{d}{dx}\Bigg(P_2(\mathcal{U}^{\rm eff})' + k_B T^{\rm eff}P_2' - \frac{k_B^2T^2a^2}{2}[\phi_0''(\mathcal{U}^{\rm eff})' + k_B T^{\rm eff}\phi_0''']'' + g\frac{k_B^2T^2a^2}{2}\phi_0''\phi_0'''\Bigg) = 0.$$

The last equation implies that

$$P_2(\mathcal{U}^{\rm eff})' + k_B T^{\rm eff}P_2' = -j_2 + \frac{k_B^2T^2a^2}{2}[\phi_0''(\mathcal{U}^{\rm eff})' + k_B T^{\rm eff}\phi_0''']'' - g\frac{k_B^2T^2a^2}{2}\phi_0''\phi_0''', \tag{B3}$$

where the current term j_2 does not depend on x. Rewriting P_2 as

$$P_2(x) = \frac{D(x)\phi_0}{(k_BT + g\phi_0)},$$

Eq. (B3) yields

$$D(x) = \int_0^x \frac{dy}{\phi_0(y)}\Bigg(\frac{k_B^2T^2a^2}{2}\Bigg\{[\phi_0''(y)(\mathcal{U}^{\rm eff})' + k_B T^{\rm eff}\phi_0'''(y)]' - \frac{g}{2}[\phi_0''(y)]^2\Bigg\}' - j_2\Bigg) + D_0. \tag{B4}$$

Now the current j_2 is determined by the condition that P_2 is a spatially periodic function [i.e., $D(x)=D(x+l)$], while the constant D_0 can be calculated from the condition $\int_0^l dx\, P_2(x)=0$. Using the relations

$$\mathcal{U}^{\rm eff} = -\frac{k_B T\phi_0'(x)}{\phi_0(x)}$$

and

$$\frac{\partial \phi_0}{\partial T} = \Bigg(-\ln\phi_0(x) + \frac{\int_0^l dy[\phi_0\ln\phi_0(y)/T^{\rm eff}(y)]}{\int_0^l dy[\phi_0(y)/T^{\rm eff}(y)]}\Bigg)\frac{\phi_0(x)}{T^{\rm eff}(x)}, \tag{B5}$$

an explicit expression for the probability current $J=j_2/\omega^2\eta^3$ follows immediately:

$$J = \frac{k_B^2T^2a^2}{2\omega^2\eta^2\left(\int_0^l dx/\phi_0\right)}\int_0^l\frac{dx}{\phi_0}\Bigg[\Bigg(-k_BT\frac{\phi_0'\phi_0''}{\phi_0} + (k_BT + g\phi_0)\phi_0'''\Bigg)' - \frac{g}{2}(\phi_0'')^2\Bigg]' + O(1/\omega^4).$$

Long algebraic manipulations yield the final result for the current, Eq. (31), reported in the text.

[1] P. Reimann, Phys. Rep. **361**, 57 (2002).
[2] See, e.g., the reviews R.D. Astumian and P. Hänggi, Phys. Today **55**(11), 33 (2002); F. Jülicher, A. Ajdari, and J. Prost, Rev. Mod. Phys. **69**, 1269 (1997); R.D. Astumian, Science **276**, 917 (1997).
[3] P. Reimann, R. Bartussek, R. Häussler, and P. Hänggi, Phys. Lett. A **215**, 26 (1996).
[4] R. Bartussek, P. Hänggi, and J.P. Kissner, Europhys. Lett. **28**, 459 (1994); M.O. Magnasco, Phys. Rev. Lett. **71**, 1477 (1993).
[5] A.L.R. Bug and B.J. Berne, Phys. Rev. Lett. **59**, 948 (1987); J. Prost, J.F. Chauwin, L. Peliti, and A. Ajdari, *ibid.* **72**, 2652 (1994).
[6] J. Rousselet, L. Salome, A. Ajdari, and J. Prost, Nature (London) **370**, 446 (1994).
[7] I. Derényi, C. Lee, and A.L. Barabási, Phys. Rev. Lett. **80**, 1473 (1998).
[8] J. F. Wambaugh *et al.*, Phys. Rev. Lett. **83**, 5106 (1999); C.-S. Lee, B. Jankó, I. Derényi, and A.-L. Barabási, Nature (London) **400**, 337 (1999); C.J. Olson, C. Reichhardt, B. Jankó, and F. Nori, Phys. Rev. Lett. **87**, 177002 (2001); F. Marchesoni, B.Y. Zhu, and F. Nori, Physica A **325**, 78 (2003); B.Y. Zhu, F. Marchesoni, and F. Nori, Physica E (Amsterdam) **18**, 318 (2003); **18**, 322, (2003); Phys. Rev. Lett. **92**, 180602 (2004); B.Y. Zhu, F. Marchesoni, V.V. Moshchalkov, and F. Nori, Phys. Rev. B **68**, 014514 (2003); Physica C **388**, 665 (2003); **404**, 260 (2004).
[9] S. Savel'ev and F. Nori, Nat. Mater. **1**, 179 (2002).
[10] S. Savel'ev, F. Marchesoni, P. Hänggi, and F. Nori, Europhys. Lett. **67**, 179 (2004); Eur. Phys. J. B **40**, 403 (2004); Phys. Rev. E **70**, 066109 (2004).
[11] S. Savel'ev, F. Marchesoni, and F. Nori, Phys. Rev. Lett. **91**, 010601 (2003).
[12] S. Savel'ev, F. Marchesoni, and F. Nori, Phys. Rev. Lett. **92**, 160602 (2004).
[13] An exception is given by Frenkel-Kontorova chains on ratchet substrates; see F. Marchesoni, Phys. Rev. Lett. **77**, 2364 (1996); G. Costantini and F. Marchesoni, *ibid.* **87**, 114102 (2001).
[14] I. Derényi and T. Vicsek, Phys. Rev. Lett. **75**, 374 (1995); excluded volume forces have been discussed also by Y. Aghababaie, G.I. Menon, and M. Plischke, Phys. Rev. E **59**, 2578 (1999).
[15] J.E. Villegas, S. Savel'ev, F. Nori, E.M. Gonzalez, J.V. Anguita, R. García, and J.L. Vicent, Science **302**, 1188 (2003).
[16] H. Risken, *The Fokker-Planck Equation* (Springer, Berlin, 1984).
[17] E.M. Lifshitz and L.P. Pitaevskii, *Physical Kinetics* (Butterworth-Heinemann, Oxford, 1999), Chap. 1.
[18] C. Van den Broeck, J.M.R. Parrondo, and R. Toral, Phys. Rev. Lett. **73**, 3395 (1994); P. Reimann *et al.*, Europhys. Lett. **45**, 545 (1999).
[19] V.S. Gorbachev and S.E. Savel'ev, JETP **80**, 694 (1995).
[20] P.M. Chaikin and T.C. Lubensky, *Principles of Condensed Matter Physics* (Cambridge University Press, Cambridge, England, 1995).
[21] A.W. Müller, Phys. Lett. **96A**, 319 (1983); Prog. Biophys. Mol. Biol. **63**, 193 (1995).
[22] L. Gammaitoni, P. Hänggi, P. Jung, and F. Marchesoni, Rev. Mod. Phys. **70**, 223 (1998); F. Marchesoni and P. Grigolini, Physica A **121**, 269 (1983).
[23] G.N. Mil'stein and M.V. Tretyakov, J. Phys. A **32**, 5795 (1999).